Tellus
SERIES A DYNAMIC METEOROLOGY AND OCEANOGRAPHY
PUBLISHED BY THE INTERNATIONAL METEOROLOGICAL INSTITUTE IN STOCKHOLM

Tellus (2011), 63A, 653–663

TELLUS

Attribution of recent changes in autumn cyclone associated precipitation in the Arctic

By JULIENNE C. STROEVE*, MARK C. SERREZE, ANDREW BARRETT and DAVID N. KINDIG, *National Snow and Ice Data Center, Cooperative Institute for Research in Environmental Science, Campus Box 449, University of Colorado, Boulder CO 80309-0449, USA*

(Manuscript received 5 April 2010; in final form 21 January 2011)

ABSTRACT

An Arctic Ocean with less sea ice and more open water in September has led to anomalous warming of the overlying atmosphere in autumn. Through influences on column water vapour and atmospheric circulation, it is reasonable to expect that this warming will have impacts on Arctic precipitation. Analysis of data from the JRA-25 atmospheric reanalysis reveals an autumn increase in cyclone-associated precipitation over the past decade. This is linked to a shift in atmospheric circulation towards more frequent and more intense cyclones in the Atlantic sector of the Arctic. Composites based on years with the five lowest and five highest September ice extents reveal more autumn cyclone associated precipitation and column water vapour during low ice years than during high ice years. However, difficulties in establishing cause and effect, including the absence of a clear association between spatial patterns of recent precipitation changes and ice extent anomalies, lead us to conclude that attribution of recent autumn precipitation increases to reduced ice cover is premature.

1. Introduction

There is broad agreement between global climate model (GCM) simulations that warming linked to rising concentrations of atmospheric greenhouse gases (GHGs) will lead to increased precipitation in northern high latitudes (e.g. Finnis et al., 2007; Kattsov et al., 2007; Deser et al., 2010). This is generally viewed in terms of the greater moisture holding capacity of a warmer atmosphere through the Clausius Clapeyron equation; with more water vapour to work with, extratropical cyclones, the major source of precipitation in this region, will tend to generate more precipitation.

Finnis et al. (2007) recently assessed projected 21st century changes in cyclone frequency and cyclone associated precipitation for different sectors of the northern hemisphere using output from the National Center for Atmospheric Research (NCAR) Community Climate System Model version 3 (CCSM3). The focus was on the cold seasons (autumn, winter and spring), comparing output from five ensemble members for the 20th century and five ensemble members for the 21st century. The dominant signal is a 21st century decrease in mid-latitude cyclone frequencies, paired with an essentially hemispheric-wide increase in the daily precipitation associated with each cyclone. This increase in cyclone 'precipitation efficiency' was explained in terms of the increase in available atmospheric moisture. In high latitudes, there is little change in cyclone frequency, such that the increase in total precipitation is driven by the increased precipitation efficiency. While few notable changes in cyclone intensity were observed (based on the Laplacian of sea level pressure (SLP) at each cyclone centre) one exception is the Greenland-Iceland-Norwegian seas sector, where intensities were found to decline.

However, as pointed out by Finnis et al. (2007) different modelling studies have come to divergent conclusions. The pairing of 21st century increases in middle and high-latitude precipitation with a general decrease in cyclone frequency is a fairly common theme. In some studies, however, this is paired with an increase in the frequency of intense cyclones (e.g. Lambert and Fyfe, 2006). In others, the frequency of intense systems declines (Sinclair and Watterson, 1999). Yet other studies find poleward shifts in storm tracks (Yin, 2005). These discrepancies may have many sources, including the use of different models with different experimental designs and sets of metrics.

Projecting how precipitation patterns and amounts will evolve in a warming climate is a particular challenge in the Arctic region, where changes in sea ice extent will alter vertical stability, moisture availability and regional baroclinicity. Although impacts of changing sea ice on circulation and precipitation are implicit in coupled model simulations, such as in the study by Finnis et al. (2007), impacts have been specifically addressed in

*Corresponding author.
e-mail: stroeve@kryos.colorado.edu
DOI: 10.1111/j.1600-0870.2011.00515.x

a number of idealized sensitivity studies (e.g. Alexander et al., 2004; Magnusdottir et al., 2004; Seierstad and Bader, 2008, Deser et al., 2010). Typically, these involve comparing control runs using 20th century sea ice conditions with runs using altered ice conditions, such as an annual cycle of ice extent for the late 21st century obtained from coupled model simulations. Conclusions range widely; while some studies indicate that impacts of reduced ice extent on circulation and/or precipitation will be largely limited to the Arctic, others point to influences extending into middle latitudes.

In light of discrepancies between different modelling studies, it is valuable to assess changes in atmospheric circulation and precipitation that have actually been observed in the Arctic. Over the past 30 yr there has been a considerable decline in summer Arctic sea ice extent (e.g. Stroeve et al., 2008). Having more open water at the end of the summer ice melt season, with more sensible heat in the ocean mixed layer, leads to stronger and more widespread vertical heat fluxes from the ocean to the atmosphere in autumn as the ocean cools and sea ice forms. Indeed, recent years have seen strong positive autumn temperature anomalies centred over regions of anomalous open water, most pronounced at the surface but also extending though a considerable depth of the troposphere (Serreze et al., 2009; Screen and Simmonds, 2010). Simmonds and Keay (2009) argue for a link between the observed downward trend in September Arctic sea ice extent and increased strength of September cyclones based on analysis of data from the Japanese 25-yr (JRA-25) atmospheric reanalysis (Onogi et al., 2005, 2007). They propose this link in terms of increased latent heat fluxes associated with more open water. Interestingly, applying output from the cyclone tracking algorithm of Serreze et al. (1997) to precipitation fields from JRA-25 (the same algorithm used in the Finnis et al. study) reveals a positive trend in autumn (September–November), cyclone-associated precipitation (CAP), with an autumn trend for the region north of 60°N of 0.33 mm yr^{-1},statistically significant at 95% (Fig. 1). An increase in cyclone-associated autumn precipitation is particularly pronounced in recent years of anomalously low ice extent (2004–2008).

However, cause and effect is unclear. Has the reduction in September sea ice extent forced circulation changes, including a tendency towards stronger cyclones and thus more autumn precipitation or has there been a shift in circulation and precipitation linked to other factors? The objective of this paper is to examine these issues for the period 1979–2008 using output from a cyclone-detection and tracking algorithm applied to JRA-25 SLP fields, along with JRA-25 fields of precipitation, column water vapour and surface fluxes.

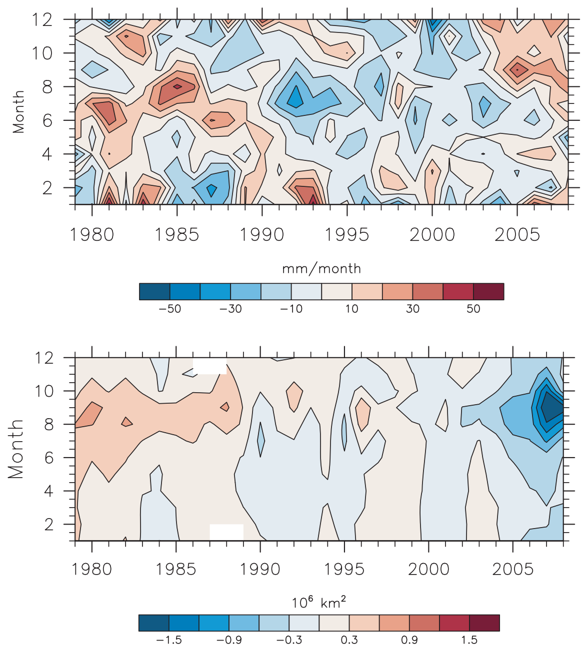

Fig. 1. Anomalies in cyclone associated precipitation by year (*x*-axis) and month (*y*-axis) for the region north of 60°N based on data from JRA-25 (top panel) and anomalies in sea ice extent based on passive microwave satellite observations (bottom panel). Anomalies are computed relative to the 1979–2008 mean. See text for methods used to calculate CAP.

2. Data

The Serreze et al. (1997) cyclone detection and tracking algorithm used here has been employed to examine Northern Hemisphere cyclone trends (McCabe et al., 2001), the tracks and deepening characteristics of cyclones in the northern North Atlantic (Tsukernik et al., 2006) and characteristics of the summer cyclone frequency maximum over the central Arctic Ocean (Serreze and Barrett, 2008). The algorithm is applied to 6-hourly Northern Hemisphere SLP fields. Cyclone detection is based on a series of search patterns, testing whether a grid point SLP value is surrounded by grid points values at least 1 hPa higher than the central point tested. Cyclone tracking employs a nearest neighbour approach that compares system positions for a given 6-h chart with those for the next 6-h chart. Two measures of cyclone intensity are provided, the cyclone central pressure and the Laplacian of SLP at the cyclone centre. Cyclone central pressure is simply the pressure at the grid point with the lowest pressure. The Laplacian, ∇^2SLP, is proportional to the relative vorticity and unlike cyclone central pressure is not influenced by the background pressure field. This paper represents the first application of the cyclone detection algorithm to JRA-25 data. Previous observational studies (e.g. Serreze et al., 1997; Tsukernik et al., 2006; Serreze and Barrett, 2008) used output based on SLP data from the NCEP (National Centers for Environmental Prediction)/NCAR reanalysis (Kalnay et al., 1996). For consistency with our earlier studies as well as the study by Simmonds and Kaey (2009), the algorithm makes use of JRA-25 SLP fields available on a 2.5 × 2.5 degree latitude/longitude grid. As mentioned, Finnis et al. (2007) made use of the same algorithm to identify cyclone centres using daily SLP fields from the CCSM3 runs.

We identify CAP using the same approach of Finnis et al. (2007). This provides for some direct comparisons with that study. The JRA-25 reanalysis provides grid point precipitation broken down into its large-scale (associated with synoptic-scale processes) and convective components. CAP is defined as the precipitation at all grid points that falls within a 250 km radius of a cyclone centre (approximately one-fourth Rossby radius), the position of which is determined from the detection and tracking algorithm just described, and for which the large-scale precipitation rate exceeds 1.5 mm d^{-1}, plus the convective precipitation within the same radius. A threshold of 1.5 mm d^{-1} allows for an adequate separation of precipitation from different weather systems without excluding regions of significant precipitation. Any convective precipitation within the 250 km radius is added back to the CAP totals. One can then add CAP at each grid cell to obtain spatial fields and regional totals (as in Fig. 1).

JRA-25 is a more recent effort than the NCEP/NCAR and European Centre for Medium-Range Weather Forecasts 40-yr (ERA-40) reanalyses. Onogi et al. (2005, 2007) provide details. Briefly, like ERA-40, the system assimilates satellite radiances rather than retrieved profiles, an approach which avoids trends and variability due to changes introduced in satellite data processing over the years. JRA-25 has higher vertical resolution than NCEP/NCAR, and assimilates both marine and terrestrial surface air temperatures. Satellite-derived sea ice is treated as fractional ice cover. The JRA-25 record begins in 1979, corresponding to the advent of modern satellite data streams.

Use of JRA-25 precipitation recognizes that the high-latitude station record is too sparse to adequately address spatio-temporal variability, particularly over the Arctic Ocean. Past studies (e.g. Serreze et al., 2005) find that precipitation distributions from reanalyses are physically consistent with patterns of atmospheric circulation variability but often have large biases. Overall performance of JRA-25 is comparable to ERA-40 (Bromwich et al., 2007). Onogi et al. (2007) found that the 6-hourly global total precipitation distribution and amount are well produced both in space and time in the JRA-25 reanalysis. As part of our study, JRA-25 grid point precipitation was compared to station records from the Global Historical Climatology Network Version 2 (GHCN) (http://www.ncdc.noaa.gov/oa/climate/ghcn-monthly/index.php). Temporal correlations between monthly precipitation from available stations north of 60°N (427 stations) and the closest JRA-25 grid point for each month from September to November range from very good ($r > 0.9$) to very poor. Good correlations (0.7–0.9) primarily occur over Eurasia. The regions of poor correlation reflect many factors, including model shortcomings, scale differences between the data sets (station versus grid point), as well as often large errors in the observations, related in part to gauge undercatch of snow. Low correlations in the Canadian Arctic, a feature also seen in comparisons between observations and ERA-40 output (Serreze et al., 2005) appear to stem from the very low precipitation in this region, such that even small observation or model errors strongly affect the time series.

3. Results

3.1. Analysis of pentads

Turning back to Fig. 1, the most recent pentad (2004–2008) has seen relatively high autumn precipitation and low summer sea ice extent, contrasting sharply with lower precipitation characterizing the immediately prior pentad of 1999–2003 or the mixed pattern of precipitation anomalies in the beginning of the data record when high September ice extents were prevalent. The recent increase in autumn CAP averaged for the region north of 60°N, however, masks considerable spatial heterogeneity. Figure 2 shows spatial patterns of autumn CAP anomalies for six pentads together with corresponding SLP anomalies. For the 2004–2008 pentad, positive anomalies in CAP are most pronounced in the Greenland and Norwegian seas and extending northeastward into the Barents and eastern Kara seas (locally >50 mm per month). Positive anomalies also characterize most land areas of Eurasia and North America as well as Baffin Bay and Davis Strait. While there are also negative anomalies (notably in Alaska, the Canadian Archipelago, eastern Siberia and the central Arctic Ocean), no other pentad exhibits positive CAP anomalies as widespread as those for 2004–2008. We stress that for all pentads, the total (large-scale and convective) precipitation patterns are nearly identical to the patterns for CAP, both in magnitude and spatial patterns. In other words, most Arctic precipitation in autumn is cyclone associated.

Autumn SLP anomalies (shown as contours in Fig. 2) for the 2004–2008 pentad are negative over the Barents Sea extending eastwards into the East Siberian Sea and positive over the Canada Basin, a pattern that broadly resembles the Arctic summer dipole anomaly discussed by Wang et al. (2009). This anomalous low-pressure area is associated with primarily positive precipitation anomalies over the Atlantic side of the Arctic and Eurasia, a feature absent in most of the prior pentads. Only in the 1979–1983 pentad do we see positive CAP anomalies over the Atlantic side of the Arctic that extend towards the Kara Sea associated with anomalously low SLP.

The CAP anomaly patterns for the different pentads are broadly consistent with anomalies in cyclone intensity (Figs 3 and 4). For example, a pattern of anomalously deep cyclones (i.e. low cyclone central pressure) extends eastwards from the Greenland and Norwegian seas towards the Barents and Kara seas for the 2004–2008 pentad (Fig. 3). The increased CAP in the North Atlantic region during the 1979–1983 pentad is similarly associated with a pattern of anomalously low cyclone pressure, whereas drier conditions tend to be associated with anomalously

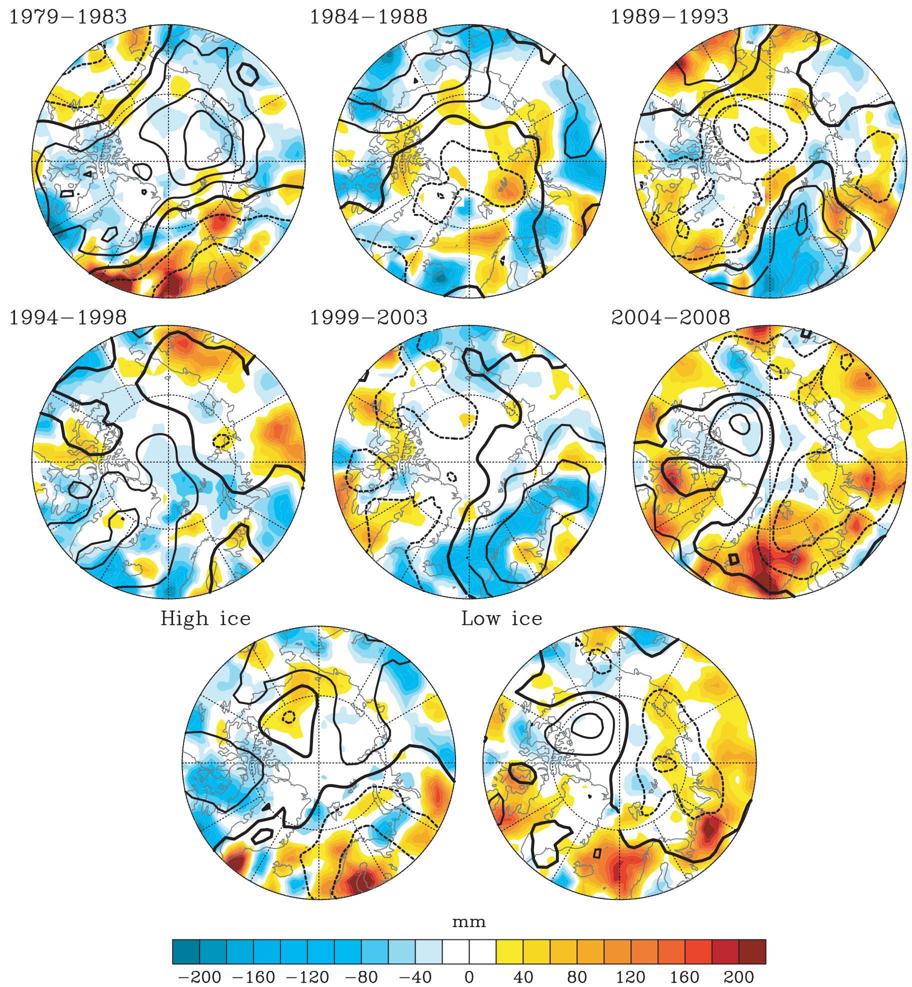

Fig. 2. Anomalies in autumn cyclone associated precipitation for different pentads and for low and high ice years. SLP anomalies are also shown (dotted isolines for negative anomalies and solid isolines for positive anomalies). Anomalies are computed relative to the 1979–2008 mean.

high cyclone central pressure. There is also general agreement between regions of more autumn CAP and anomalously strong cyclones, as defined by the Laplacian of SLP at the cyclone centres. Specifically, more intense cyclones are located in the Greenland, Norwegian, Barents and Kara seas during the last pentad (Fig. 4) where the largest positive CAP anomalies are found. More intense cyclones are also observed over regions of North America and Eurasia, again in agreement with an increase in CAP. The peak positive CAP anomaly for the most recent pentad east of Iceland is seen to be more closely linked to cyclone intensity from the Laplacian measure as compared to cyclone central pressure.

3.2. *Analysis of low versus high ice years*

To directly examine relationships between sea ice extent and CAP, we compiled composites based on the 5 yr with the highest September sea ice extent (1980, 1983, 1986, 1992, 1996: mean extent of 7.7 million km^2) and the 5 yr with the lowest extent (2002, 2005, 2006, 2007, 2008: mean extent of 5.3 million km^2) (Fig. 2, bottom two panels). While the CAP anomalies for low ice years show a rather similar anomaly pattern to the most recent pentad (this follows in that the two composites have all but 1 yr in common), the overall magnitude of increased CAP is generally smaller than observed during the 2004–2008 pentad. Compared to low ice years, conditions for high ice years are generally drier in the Greenland, Norwegian, Barents and Kara seas as well as over most of Eurasia and North America. Wetter than normal conditions during high ice years are mostly found over Scandinavia, southwestern Eurasia and somewhat less so in the Beaufort, Chukchi and E. Siberian seas.

The SLP anomaly pattern for the five years with the lowest September ice extent (Fig. 2 bottom right-hand side) is of course also similar to the last pentad, but the negative SLP anomalies are less pronounced. This reflects the negative phase of the Northern Annular Mode that characterized autumn 2002, associated with a weaker and southward-shifted North Atlantic storm track compared to normal conditions.

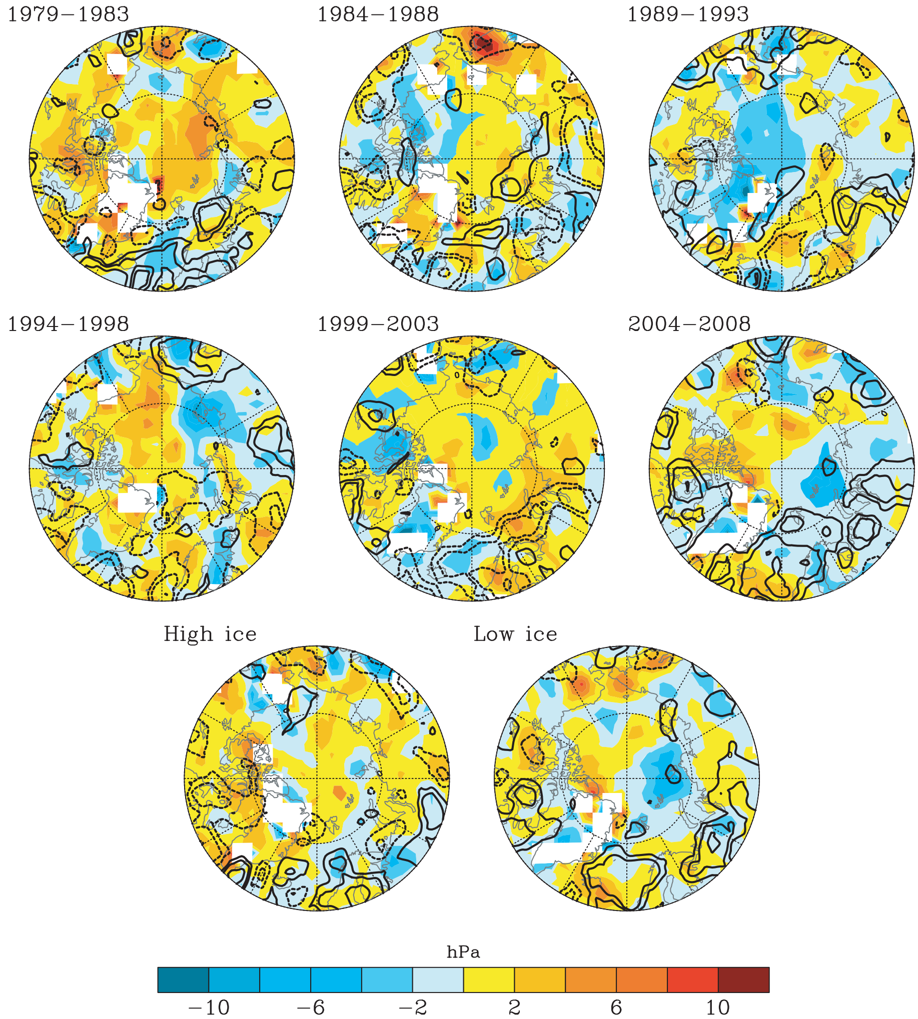

Fig. 3. Anomalies in autumn cyclone central pressure for different pentads and for low and high ice years. CAP anomalies are also shown (dotted isolines for negative anomalies, solid isolines for positive anomalies). Anomalies are computed relative to the 1979–2008 mean. Missing values are shown in white.

Cyclone central pressures are lower in the Barents and Kara Seas during low ice years, consistent with slightly higher autumn CAP in this region. Yet, compared to the last pentad the cyclones are overall weaker and less intense. As observed during the last pentad, the Laplacian of SLP at cyclone centres indicates more intense cyclones in the Icelandic and Greenland seas during low ice years, the location of the largest positive anomalies in autumn CAP during the five lowest ice years. An increase in cyclone intensity as measured by the Laplacian of SLP at cyclone centres over Scandinavia appears to help explain the increase in CAP observed in this region during high ice years.

3.3. Precipitation frequency and output

To gain further insight, we evaluate contrasts between the last two pentads of starkly opposing CAP anomalies (2004–2008 versus 1999–2003) and for the low and high ice extent years in the contributions to CAP from dynamic and thermodynamic processes. Again following Finnis et al. (2007), we derive normalized differences in mean autumn CAP associated with differences in cyclone frequency as

$$\mathrm{CAP}_{\mathrm{frequency}} = \overline{\mathrm{CAP}}_{\mathrm{high}} * [n_{\mathrm{low}} - n_{\mathrm{high}}],$$

where the number of cyclone centres for high (or the 1999–2003 pentad) and low (or the 2004–2008 pentad) ice years are given as n_{high} and n_{low}, respectively, and the mean precipitation per event for the high ice years is given as $\overline{\mathrm{CAP}}_{\mathrm{high}}$. The units are in millimetres and positive values indicate a higher frequency of events for the low ice years.

Similarly, the normalized difference in mean seasonal cyclone output (a measure of the difference in precipitation ‘efficiency’

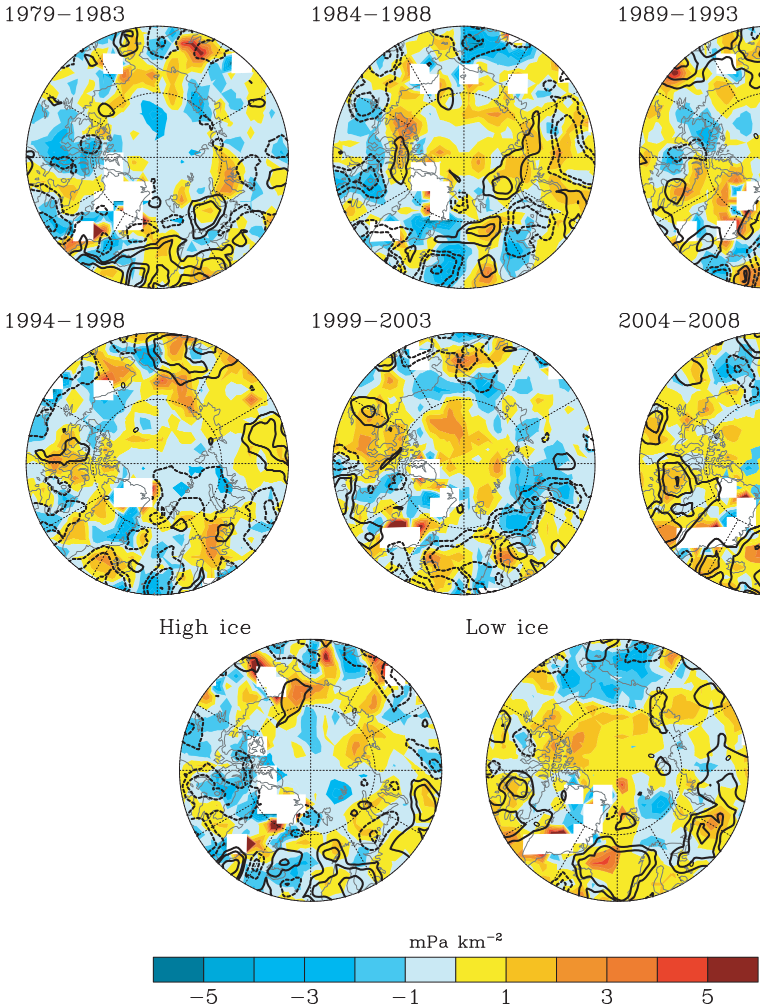

Fig. 4. Anomalies in autumn cyclone intensity (Laplacian of SLP at cyclone centers) for different pentads and for low and high ice years. CAP anomalies are also shown (dotted isolines for negative anomalies, solid isolines for positive anomalies). Anomalies are computed relative to the 1979–2008 mean. Missing values are shown in white.

of cyclones) is defined as

$$\mathrm{CAP}_{\mathrm{output}} = n_{\mathrm{high}} * [\overline{\mathrm{CAP}_{\mathrm{low}}} - \overline{\mathrm{CAP}_{\mathrm{high}}}].$$

As discussed by Finnis et al. (2007), the frequency term is a reflection of changing atmospheric circulation (cyclone frequency) whereas the output term reflects precipitation changes from changes in cyclone processes or atmospheric state that affect the precipitation rate.

The normalized mean seasonal cyclone frequency and output are averaged over several regions (Fig. 5) that roughly capture the CAP anomaly patterns for the low ice years (Fig. 2). They comprise the high-latitude North America (HNA), the Chukchi and E. Siberian seas (CHU), Central Russia (CRU), the Greenland, Norwegian and Barents seas (GNB), Greenland (GRE) and all areas north of 80°N (TOP). Additionally, we compute results for the entire Arctic region north of 60°N (ARC) and the Greenland central Russia region (GCR), which combine both the CRU and GNB regions.

The total CAP difference between the two pentads for each region is the sum of the difference in cyclone output (light grey) and frequency (dark grey). For most regions, there is a positive contribution from both components, that is, both components contribute to higher total CAP during the most recent pentad (Fig. 6, top panel). This is not surprising, for within an environment conducive to stronger cyclones (tending to yield more precipitation) it is reasonable to expect more cyclones as well. Exceptions are the GRE region, where increased output is partly countered by lower frequency, and TOP, where output is lower and the change in frequency is near zero. In the GNB region, more frequent cyclones play the dominant role in the observed CAP anomalies.

A somewhat different story emerges when comparing composites for the five highest and five lowest September ice extent

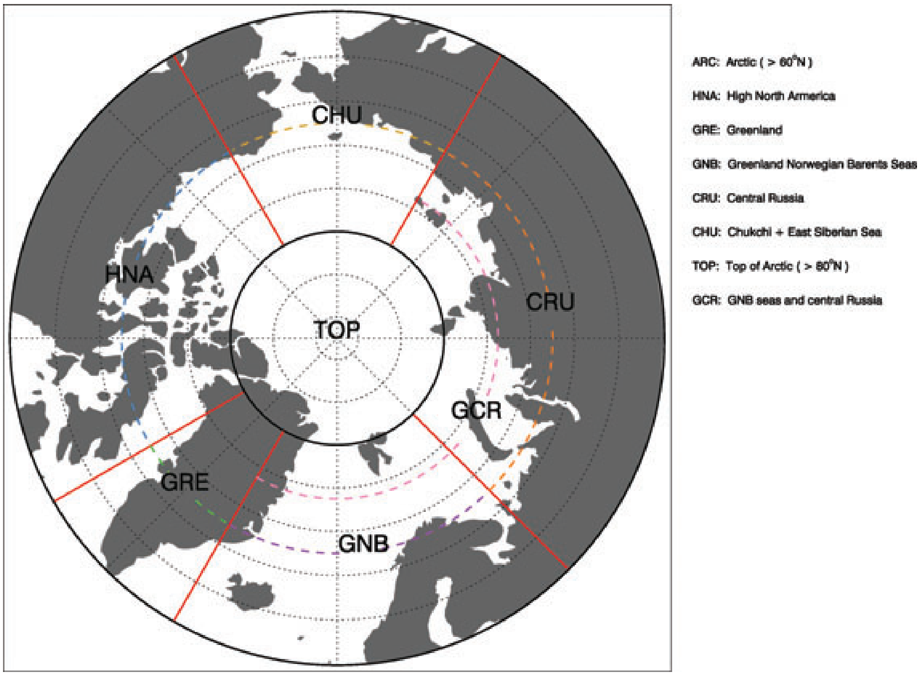

Fig. 5. Regions over which cyclone-associated precipitation are aggregated, comprising the high-latitude North America (HNA), the Chukchi and East Siberian seas (CHU), Central Russia (CRU), the Greenland, Norwegian and Barents seas (GNB), Greenland (GRE) and all areas north of 80°N (TOP). Additionally, we compute results for the entire Arctic region north of 60°N (ARC) and the Greenland central Russia region (GCR) which combines both the CRU and GNB regions.

years (Fig. 6, bottom panel). In the GNB region, the effects of changes in cyclone frequency and cyclone efficiency oppose each other—while there is an increase in mean cyclone output during low ice years in this region, this is partially offset by a small decrease in cyclone frequency. The Chukchi/Siberian (CHU) region on the other hand shows an increase in cyclone frequency more than offset by a decrease in mean storm output, yielding less total CAP in that region during low ice years. Averaged for the Arctic region as a whole, the contributions to increased CAP during low ice years from frequency and efficiency are similar. To the extent that one can justify a comparison between our results and those of Finnis et al. (2007), which looked at 21st century changes over an extended cold season (September–May), the JRA-25 data suggest mixed contributions from changing storm frequency and output in contrast to a dominant role of increased output in the Finnis et al. (2007) study.

Regional increases in cyclone efficiency as assessed from the JRA-25 data could be related to increased cyclone intensity, increased availability of water vapour or other processes that enhance precipitation. As discussed, Figs 3 and 4 show increased cyclone intensity in regions of enhanced autumn CAP during recent years of low September sea ice concentration. The large areas of open water during low ice years at the end of the summer melt season have fostered stronger sensible and latent heat transfers from the surface to the atmosphere in autumn, which would be conducive to increased cyclone intensity. Anomalies of latent and sensible heat fluxes for the low ice years and high ice years show the effect of open water very clearly (Fig. 7 top and middle panels). During the low ice years, positive anomalies in the turbulent fluxes characterize areas of anomalous open water, namely the Beaufort, Chukchi, E. Siberian and Laptev seas. Anomalies for the high ice years in these same areas are negative. Interestingly, for both the low and high ice years, positive flux anomalies characterize the northern North Atlantic (which is always ice-free). This could be associated with increased ocean heat flux (e.g. Orvik and Skagseth, 2005). Precipitable water (column water vapour) (Fig. 7 bottom panels) is higher over nearly all of the regions north of 60°N during low as compared to high ice years (consistent with a general warming of the Arctic troposphere), but with the largest positive anomalies located in the Chukchi and East Siberian seas linked to anomalous open water. Yet this is not the region of the largest positive anomalies in autumn CAP, and in fact is characterized by both positive (E. Siberian Sea) and negative (Chukchi Sea) precipitation anomalies.

4. Summary and discussion

Climate models project that Arctic precipitation will show a general increase through the 21st century, in large part because of the greater moisture holding capacity of a warmer atmosphere.

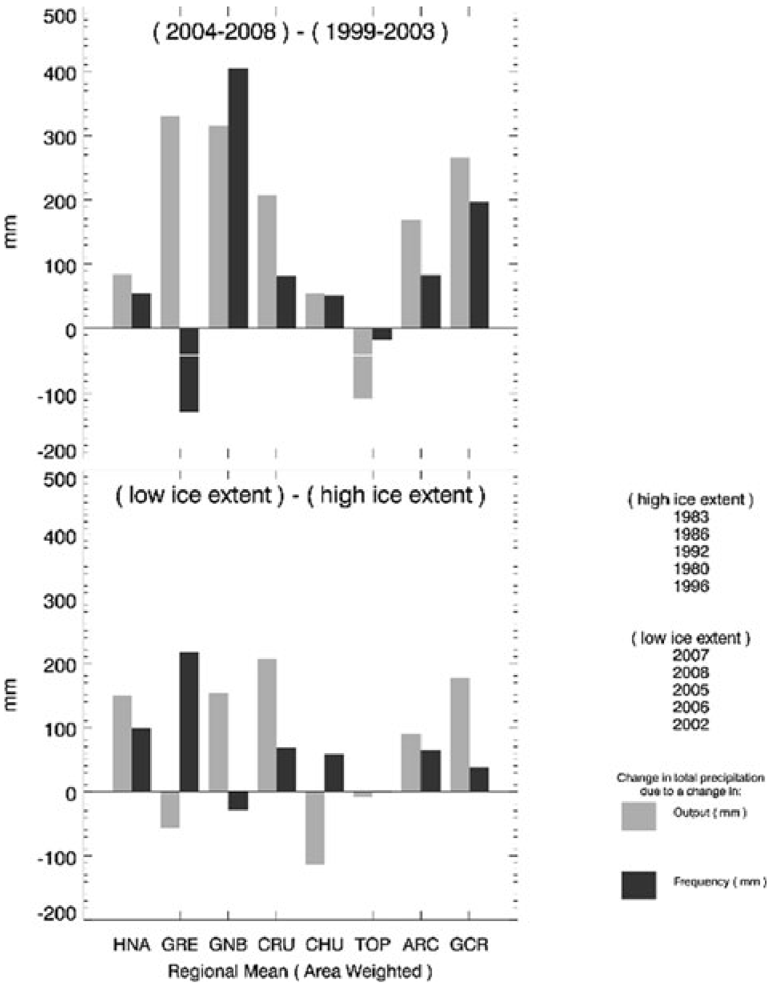

Fig. 6. Differences in autumn cyclone associated precipitation (mm) between years the 2004–2008 and 1999–2003 pentad (top panel) and for low September sea ice extent and high September sea ice extent (bottom panel). Results are given for both mean cyclone output and cyclone frequency.

Other studies have argued that loss of the sea ice cover will influence patterns of precipitation and atmospheric circulation within and potentially beyond the Arctic. Based on assessments of JRA-25 data, Simmonds and Keay (2009) suggest that more open water in September has led to stronger latent and sensible heat fluxes contributing to stronger Arctic cyclones. The JRA-25 data in turn point to an increase in autumn CAP over the past decade. Can we attribute this increase to reduced sea ice extent? The answer appears to be a qualified no.

Differences in CAP and total precipitation between the two most recent pentads (1999–2003, 2004–2008) of the JRA-25 record are clearly associated with a shift in atmospheric circulation, with the 2004–2008 pentad characterized by anomalous low pressure over the Barents Sea extending eastwards into the E. Siberian Sea. This is reflected in regional increases in cyclone frequency and cyclone intensity, as well as an Arctic-wide increase in column water vapour. The latter two changes are consistent with the tendency for higher precipitation efficiency of cyclones for most (not all) areas in which CAP has increased. The tendency towards regional increases in cyclone intensity is consistent with findings from Simmonds and Keay (2009). The composite autumn CAP anomaly pattern based on the 5 yr with the lowest September sea ice extent is quite similar to the pattern for the most recent pentad (expected as the two composites have four of their five years in common), but are quite different than the composite CAP anomaly pattern for the 5 yr with the highest September sea ice extent.

The links identified between anomalies in precipitation, sea ice extent, cyclone intensity and column water are certainly intriguing. However, we see no compelling reason to argue for a forcing from reduced sea ice extent. It may be that the results can be more simply interpreted as documenting a circulation shift independent of any forcing by sea ice change. Note in this regard that while the most pronounced open water anomalies in September in recent years have been north of Alaska and eastern Siberia (e.g. Stroeve et al., 2005, 2008), in turn associated with strong positive autumn anomalies in sensible and latent heat fluxes as well as column water vapour, positive precipitation anomalies have actually been largest in the Greenland, Norwegian, Barents and Kara seas.

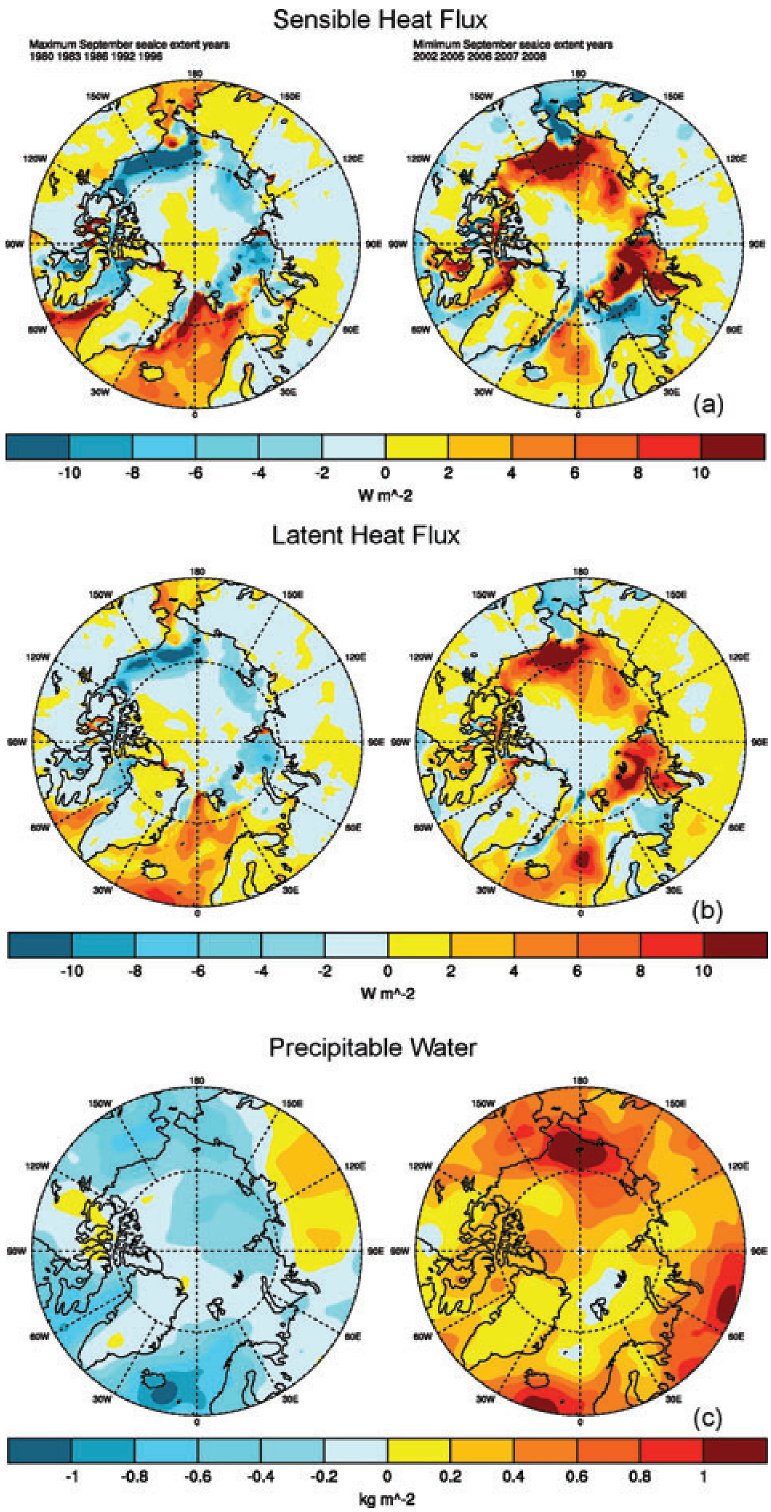

Fig. 7. Autumn anomalies of sensible heat flux, latent heat flux and precipitable water for the high (left-hand side) and low (right-hand side) ice years. Anomalies are computed relative to the 1979–2008 mean. Fluxes are defined as positive upwards.

Our study nevertheless raises a number of issues. An obvious one is that our interpretations in large part depend on the veracity of precipitation and turbulent flux estimates from JRA-25. As a future effort, it may be insightful to examine recent changes in Arctic precipitation and energy fluxes with ERA-Interim, the newest reanalysis from the European Center for Medium Range Weather Forecasts that extends back to 1989 (http://www.ecmwf.int/research/era/do/get/index), and

MERRA, the newest reanalysis from NASA which extends back to 1979 (http://gmao.gsfc.nasa.gov/research/merra/). Second, cause and effect cannot be separated from a purely observational perspective such as ours; the possibility that altered sea ice cover has in fact forced part of the observed circulation change hence cannot be entirely dismissed. It is notable in this regard that at least two recent observational studies besides Simmonds and Keay (2009) cite evidence of circulation anomalies following Septembers with low ice extent (Francis et al., 2009; Overland and Wang, 2010).

A third issue is that apart from a general increase in high latitude precipitation, there is limited agreement between existing modelling studies as to the changes in circulation, cyclone frequency, intensity and cyclone-associated precipitation that can be expected in a greenhouse warmed world, let alone signals linked to attendant changes in sea ice. An effective comparison between observed and expected change will require a coordinated set of simulations with different models each adopting the same experimental design, and assessments of the ability of different models to reproduce physical processes driving precipitation variability in the Arctic.

5. Acknowledgments

This study was supported by National Science Foundation grants ARC 0805821, ARC 0901962 and National Aeronautics and Space Administration grants NNX08AQ70G and NNG04GO51G.

References

Alexander, M. A., Bhatt, U. S., Walsh, J. E., Timlin, M. S., Miller, J. S. and co-authors. 2004. The atmospheric response to realistic Arctic sea ice anomalies in an AGCM during winter. *J. Clim.* **17**, 890–905.

Bromwich D. A., Fogt, R. L., Hodges, K. I. and Walsh, J. E. 2007. A tropospheric assessments of the ERA-40, NCEP, and JRA-25 global reanalyses in the polar regions. *J. Geophys. Res.* **112**, D10111, doi:10.1029/2006JD007859.

Deser, C., Tomas, R., Alexander, M. and Lawrence, D. 2010. The seasonal atmospheric response to projected Arctic sea ice loss in the late twenty-first century. *J. Clim.* **23**, 333–351.

Finnis, J., Holland, M. M., Serreze, M. C. and Cassano, J. J. 2007. Response of Northern Hemisphere extratropical cyclone activity and associated precipitation to climate change, as represented by the Community Climate System Model. *J. Geophys. Res.* **112**, G04S42, doi:10.1029/2006JG000286.

Francis, J. A., Chan, W., Leathers, D. J., Miller, J. R. and Veron, D. E. 2009. Winter Northern Hemisphere weather patterns remember summer Arctic sea ice extent. *Geophys. Res. Lett.* **36**, L07503, doi:10.1029/2009GL037274.

Kalnay, E., Kanamitsu, M., Kistler, R., Collins, W., Deaven, D. and co-authors. 1996. The NCEP/NCAR 40-year reanalysis project. *Bull. Am. Meteorol. Soc.* **77**, 437–471.

Kattsov, V. M., Walsh, J. E., Chapman, W. L., Govorkova, V. A., Pavlova, T. V. and co-authors. 2007. Simulation and projection of Arctic freshwater budget components by the IPCC AR4 Global Climate Models. *J. Hydrometeorol.* **8**, 571–589, doi:10.1175/JHM575.1.

Lambert, S. J. and Fyfe, J. C. 2006. Changes in winter cyclone frequencies and strengths simulated in enhanced greenhouse warming experiments: results from models participating in the IPCC diagnostic exercise. *Clim. Dyn.*, **26**, 713–728.

Magnusdottir, G., Deser, C. and Saravanan, R. 2004. The effects of North Atlantic SST and sea ice anomalies on the winter circulation in CCSM3, Part I: main features and storm track characteristics of the response. *J. Clim.* **17**, 857–876.

McCabe, G. J., Clark, M. P. and Serreze, M. C. 2001. Trends in Northern Hemisphere surface cyclone frequency and intensity. *J. Clim.* **14**, 4351–4362.

Onogi, K., Koide, H., Sakamoti, M., Kobayashi, S. and co-authors 2005. JRA-25: Japanese 25-year re-analysis project – progress and status. *Quart. J. Roy. Meteorol Soc.* **131**, 3259–3268.

Onogi, K., Tsutsui, J., Koide, H., Sakamoto, M., Kobayashi, S. and co-authors. 2007. The JRA-25 reanalysis. *J. Met. Soc. Japan* **85**, 369–432.

Orvik, K. A. and Skagseth, O. 2005. Heat flux variations in the eastern Norwegian Atlantic Current toward the Arctic from moored instruments, 1995–2005, *Geophys. Res. Lett.* **32**, L14610, doi:10.1029/2005GL023487.

Overland, J. E. and Wang, M. 2010. Large-scale atmospheric circulation changes are associated with the recent loss of Arctic sea ice. *Tellus* **62A**, 1–9.

Screen, J. A. and Simmonds, I. 2010. The central role of diminishing sea ice in recent Arctic temperature amplification. *Nature* **464**, 1334–1337, doi:10.1038/nature09051, 2010

Seierstad, I. A. and Bader, J. 2008. Impact of a projected future Arctic sea ice reduction of extratropical storminess and the NAO. *Clim. Dyn.*, **33**, doi:10.1007/s00382-008-0463-x.

Serreze, M. C. and Barrett, A. P. 2008. The summer cyclone maximum over the central Arctic Ocean. *J. Clim.* **21**, 1048–1065.

Serreze, M. C., Carse, F., Barry, R. G. and Rogers, J. C. 1997. Icelandic low cyclone activity: climatological features, linkages with the NAO, and relationships with recent changes in the Northern Hemisphere circulation. *J. Clim.* **10**, 453–464.

Serreze, M. C., Barrett, A. and Lo, F. 2005. Northern high latitude precipitation as depicted by atmospheric reanalyses and satellite retrievals. *Mon. Wea. Rev.* **113**, 3407–3430.

Serreze, M. C., Barrett, A. P., Stroeve, J. C., Kindig, D. N. and Holland, M. M. 2009. The emergence of surface-based Arctic amplification. *The Cryosphere* **3**, 11–19.

Simmonds, I. and Keay, K. 2009. Extraordinary September Arctic sea ice reductions and their relationships with storm behavior over 1979–2008. *Geophys. Res. Lett.* **36**, L19715, doi:10.1029/2009GL039810.

Sinclair, M. R. and Watterson, I. G. 1999. Objective assessment of extratropical weather systems in simulated climates. *J. Clim.* **12**, 3467–3485.

Stroeve, J. C., Serreze, M. C., Fetterer, F., Arbetter, T., Meier, W. and co-authors. 2005. Tracking the Arctic's shrinking ice cover: another extreme September minimum in 2004. *Geophys. Res. Lett.* **32**, L04501, doi:10.1029/2004GL021810, 2005.

Stroeve, J., Serreze, M., Drobot, S., Gearheard, S., Holland, M. and co-authors. 2008. Arctic sea ice extent plummets in 2007. *EOS Trans., Am. Geophys. Soc.* **89**, 13–14.

Tsukernik, M., Kindig, D. and Serreze, M. C. 2006. Characteristics of winter cyclone activity in the northern North Atlantic: insights from observations and regional modeling. *J. Geophys. Res.* **112**, D03101, doi:10.1029/2006JD007184.

Wang, J. J., Zhang, E. Watanabe, M., Ikeda, K., Mizobata, J. E. and co-authors. 2009. Is the Dipole Anomaly a major driver to record lows in Arctic summer sea ice extent? *Geophys. Res. Lett.* **36**, L05706, doi:10.1029/2008GL036706.

Yin, J. H. 2005. A consistent poleward shift of the storm tracks in simulations of 21st century climate. *Geophys. Res. Lett.* **32**, L18701, doi:10.1029/2005GL023684.